

# Organic-templated silica membranes

## I. Gas and vapor transport properties

G. Xomeritakis<sup>a</sup>, S. Naik<sup>a</sup>, C.M. Braunbarth<sup>a</sup>, C.J. Cornelius<sup>b</sup>,  
R. Pardey<sup>c</sup>, C.J. Brinker<sup>a,b,\*</sup>

<sup>a</sup> NSF Center for Microengineered Materials, The University of New Mexico, Albuquerque, NM 87106, USA

<sup>b</sup> Advanced Materials Laboratory, Sandia National Laboratories, 1001 University Blvd. SE, Suite 100, Albuquerque, NM 87106, USA

<sup>c</sup> PDVSA Intevep, P.O. Box 76343, Caracas 1070-A, Venezuela

Received 15 August 2002; received in revised form 2 December 2002; accepted 14 December 2002

### Abstract

A novel and efficient method for molecular engineering of the pore size and porosity of microporous sol–gel silica membranes is demonstrated in this communication. By adding a suitable organic template (e.g. tetraethyl- or tetrapropylammonium bromide) in polymeric silica sols, otherwise known to result in microporous membranes with pores in the range 3–4 Å, we can ‘shift’ the pore size to 5–6 Å, as judged by single-component gas and vapor permeation results with probe molecules of increasing kinetic diameter ( $d_k$ ). The templated membranes exhibit permeances as high as  $10^{-7}$  to  $10^{-6}$  mol m<sup>-2</sup> s<sup>-1</sup> Pa<sup>-1</sup> for molecules with  $d_k < 4.0$  Å (e.g. CO<sub>2</sub>, N<sub>2</sub>, CH<sub>4</sub>), coupled with single-component selectivities of 100–1800 for N<sub>2</sub>/SF<sub>6</sub>, 20–40 for *n*-butane/*iso*-butane, and 10–20 for *para*-xylene/*ortho*-xylene. The transport properties of the templated membranes are distinctly different from those of the respective silica membranes prepared without templating, and resemble somewhat the transport properties of polycrystalline zeolite MFI membranes prepared by the lengthy, batch hydrothermal synthesis approach, using tetrapropylammonium bromide as a structure directing agent.

© 2003 Elsevier Science B.V. All rights reserved.

**Keywords:** Zeolite; Tetrapropylammonium bromide; Sol–gel silica

### 1. Introduction

Inorganic membranes with good thermal, chemical and mechanical stability have attracted considerable attention due to their potential applications in gas and vapor separations at elevated temperatures under harsh conditions [1]. Microporous inorganic membranes, such as polycrystalline zeolite, amorphous carbon and sol–gel silica comprise a particularly important

category of inorganic membranes, useful for a variety of separations including permanent gases or hydrocarbon isomers, based on differences in diffusivities and/or adsorption strengths of mixture components in membrane pores [2].

Polycrystalline zeolite membranes made by direct or seeded hydrothermal growth on porous ceramic or metallic supports have attracted considerable attention during the last decade, on account of very exciting transport properties and the potential for a variety of separations including O<sub>2</sub>/N<sub>2</sub> [3], CO<sub>2</sub>/N<sub>2</sub> [4], linear/branched paraffins [5], C<sub>8</sub> aromatics [6], saturated/unsaturated hydrocarbons [7] and water/alcohol

\* Corresponding author. Tel.: +1-505-272-7627;

fax: +1-505-272-7336.

E-mail address: cjbrink@sandia.gov (C.J. Brinker).

mixtures [8]. Carbon membranes prepared by pyrolysis of polymeric precursor films deposited on porous supports have shown potential for gas/vapor separations based on either size (e.g. CO<sub>2</sub>/CH<sub>4</sub>) or adsorption (e.g. H<sub>2</sub>/hydrocarbons) differences of mixture components in membrane micropores [9,10]. Despite their exciting transport properties, several technical problems may limit the usefulness of zeolite or carbon molecular sieve membranes for commercial applications. These include poor processibility and scalability, low permeation fluxes due to large thicknesses (usually >1 μm), and compromised selectivities due to susceptibility to cracking or undesirable intercrystalline porosity.

Sol–gel derived silica membranes represent another class of microporous molecular sieve membranes that can offer considerable advantages compared to zeolite or carbon membranes. They are typically processed using a simple dip-coating step at ambient conditions, their thickness can be controlled easily in the range 20–100 nm to improve permeation flux, and their pore size and porosity can be fine-tuned by the sol chemistry to obtain the desired separation function [11,12].

Silica membranes are typically prepared by dip-coating a suitable support in a polymeric silica sol made by acid-catalyzed hydrolysis and condensation of tetraethyl orthosilicate (TEOS), Si(OCH<sub>2</sub>CH<sub>3</sub>)<sub>4</sub>, in ethanol [13,14]. During deposition, preferential evaporation of ethanol results in the formation of a xerogel film on the surface of the support, via interpenetration and collapse of the fractal siliceous clusters contained in the sol, whereas water molecules trapped between neighboring clusters result in the formation of micropores in the size range 3–4 Å, after complete drying.

In principle, pores with larger size can be created by molecular templating, e.g. incorporation of organic molecules in the silica network that, after calcination, create pores that mimic the size and shape of the original template. One way to introduce these template molecules is by co-reacting TEOS with an organic-substituted alkoxy silane, R'-Si(OR)<sub>3</sub>, where the organic group R' is non-hydrolyzable and can be incorporated in the silica framework covalently bonded to Si atoms as a pendant ligand [15–17].

In this work we demonstrate a more elegant method for templating sol–gel silica membranes, by simply adding tetra-alkylammonium bromide salts in the polymeric silica sol prior to membrane deposition.

Such organic molecules are widely used as structure-directing agents in zeolite synthesis in powder or membrane form (e.g. tetrapropylammonium bromide, TPABr, in case of MFI) and hence, could serve as a suitable template for formation of 'zeolite-like' amorphous silica membranes with pore size close to that of zeolite MFI, e.g. ~5.5 Å [18]. Such membranes may combine properties unprecedented by polycrystalline zeolite or amorphous carbon membranes, such as good processibility, thickness <100 nm, and absence of undesirable intercrystalline porosity.

In what follows, we present preliminary results on the transport properties of different gas and vapor probe molecules of increasing kinetic diameter, e.g. CO<sub>2</sub> (3.3 Å), N<sub>2</sub> (3.64 Å), CH<sub>4</sub> (3.8 Å), *n*-butane (4.3 Å), *iso*-butane (5.0 Å), SF<sub>6</sub> (5.5 Å), *para*-xylene (5.8 Å) and *ortho*-xylene (6.8 Å), through these novel membranes and establish the role of the template by comparison with literature data of polycrystalline zeolite MFI and respective non-templated sol–gel silica membranes.

## 2. Experimental

### 2.1. Silica sol preparation

The polymeric silica sols used for membrane deposition were prepared by a two-step acid-catalyzed hydrolysis and condensation of TEOS in ethanol. In the first-step, a mixture of initial molar composition (A): TEOS–EtOH–H<sub>2</sub>O–HCl = 1.0–3.8–1.1–5 × 10<sup>-5</sup> was reacted for 90 min at 60 °C to form a stock sol which was stored in a –30 °C freezer [14]. Subsequently, additional H<sub>2</sub>O, HCl and template (TEABr or TPABr) were added to the stock sol (warmed to room temperature), to form a sol of molar composition (B): TEOS–EtOH–H<sub>2</sub>O–HCl = 1.0–3.8–5.0–1 × 10<sup>-2</sup> while the amount of template varied from 2 to 10 wt.% of the sol + template mixture [18]. Standard, non-templated silica membranes were prepared by adding H<sub>2</sub>O and HCl (but no template) to the stock sol to form a sol of molar composition (C): TEOS–EtOH–H<sub>2</sub>O–HCl = 1.0–3.8–5.0–4 × 10<sup>-3</sup> [14]. Intermediate mesoporous silica sub-layers were prepared by addition of 4 wt.% C<sub>6</sub>-surfactant (C<sub>6</sub> = hexyltriethylammonium bromide) to a sol of composition (C), resulting in a

0.125 M C<sub>6</sub>-surfactant-templated silica sol [14]. All sols were aged for 24 h at 50 °C, diluted by twice their volume with ethanol and filtered through 0.2 μm syringe filters prior to dip-coating, except for the case of the C<sub>6</sub>-surfactant templated sol where no aging was employed. It is noted that the acid amount in sols (B) and (C) was adjusted appropriately so that both sols have comparable gelation times of ~120 h ( $t_{\text{aging}}/t_{\text{gelation}} = 0.2$ ).

## 2.2. Membrane preparation

The membrane supports were 250 mm-long asymmetric alumina Membralox tubes (US Filter) of 7 mm i.d., 10 mm o.d. and a final inner layer of 50 Å γ-Al<sub>2</sub>O<sub>3</sub>. Tube segments of 5.5 cm length were initially dip-coated in the 0.125 M C<sub>6</sub>-surfactant-templated silica sol to form a smooth mesoporous sub-layer between the γ-Al<sub>2</sub>O<sub>3</sub> top layer of the tubular support and the subsequently deposited microporous membrane layer [14]. All depositions were carried out in a laminar flow chamber with circulating flow of filtered air under class-10 clean room conditions. The support tubes were dipped in the sol in a vertical position, maintained submerged for 30 s, and then withdrawn at a speed of 76 mm/min with the aid of a variable-speed linear translation stage (Industrial Devices Corp.). After withdrawal, the membranes were dried for 15 min inside the chamber and subsequently for 6 h at 120 °C in a vacuum oven. After drying, they were calcined for 3 h at 450 °C in air, 6 h at 300 °C in vacuum or 6 h at 400 °C in argon for the mesoporous, non-templated and templated, microporous membranes, respectively. The heating and cooling rates in all drying and calcination steps were 1 °C/min. Prior to permeation measurements, the membrane tube ends were glazed with epoxy glue (Duraseal, Cotronics Corp.) to repair any defects resulting from the tube cutting step.

## 2.3. Gas and vapor permeation

Single-component gas and vapor permeation measurements were conducted using a stainless steel tube-and-cell membrane holder with Viton end seals, as described in detail elsewhere [14]. For fast-permeating gases (CO<sub>2</sub>, N<sub>2</sub>, CH<sub>4</sub>), the feed was introduced at a flow rate of 50–100 sccm in the inner side of the tubular membrane at a pressure of 50–100 kPa above am-

bient. The flow rate of the permeate stream exiting the cell side of the membrane holder at ambient pressure was measured with a soap-film flowmeter. For slow-permeating components (*n*-butane, *iso*-butane, SF<sub>6</sub>; N<sub>2</sub> and CH<sub>4</sub> for the non-templated silica membranes), a Wicke–Kallenbach operation mode was employed where the feed stream and a sweep stream (He or N<sub>2</sub>) were introduced at 50–100 sccm in a counter-current flow mode from respective sides of the membrane holder at ambient pressure. Composition analysis of the permeate stream exiting the cell side of the membrane holder was performed online with the aid of a HP 5890 gas chromatograph equipped with TCD/FID and packed columns (Hayesep D 100/120 for N<sub>2</sub>, CH<sub>4</sub> and SF<sub>6</sub>; 0.19% picric acid on Graphpac, 80/100, for butane isomers, Alltech).

Vapor permeation measurements with xylene isomers were conducted in the Wicke–Kallenbach mode using a set-up described elsewhere [6,7]. The inner side of the tubular membrane was flushed with a helium carrier stream of 50 sccm, passing through saturators of respective liquid xylenes maintained at 25 °C. In this way, the partial pressure of xylene vapors in the feed was ~0.9 kPa for *para*-xylene and ~0.7 kPa for *ortho*-xylene. The cell side was flushed with a pure helium stream at 10–100 sccm and its composition in permeated xylene vapors was analyzed online with a HP 5890 gas chromatograph equipped with FID and a packed column (5% AT-1200 + 1.75% Bentone 34 on Chromosorb W-AW, 100/120, Alltech).

In all permeation experiments, the flow rates of the feed and sweep streams were regulated with the aid of thermal mass flow controllers (MKS Instruments) and monitored with soap-film flowmeters. The temperature of the membrane was controlled with a heating tape wrapped around the membrane holder and connected to a Varian power supply, and monitored with a type K thermocouple connected to a digital readout (Omega).

## 3. Model for organic-templated microporous membrane

The concept of templating can be envisioned better by considering the schematic in Fig. 1, as pointed out earlier by Brinker and coworkers [15,17]. Fig. 1(a) represents the original non-templated membrane possessing pores of initial size  $d_0$  (solvent-templated

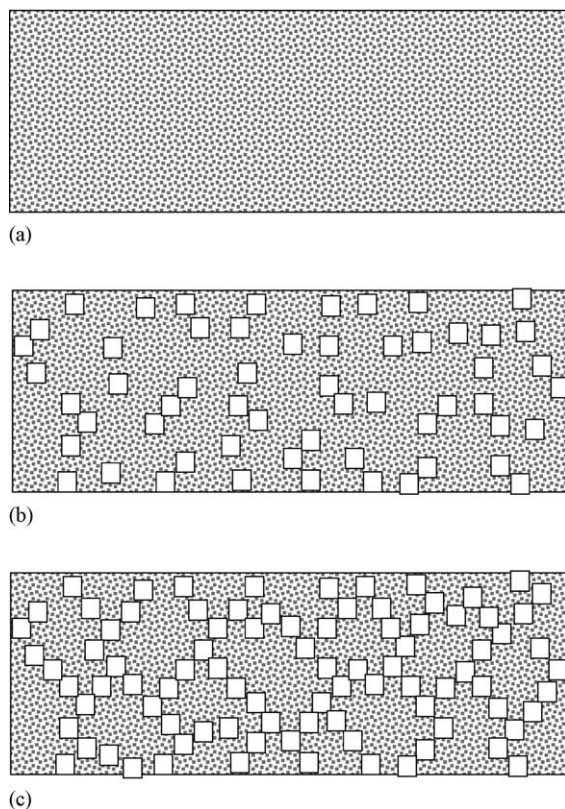


Fig. 1. Schematic representation of organic-templating approach in microporous sol-gel silica membranes: (a) original, non-templated membrane; (b) templated membrane before percolation; (c) templated membrane after percolation.

pores). After dispersing a suitable organic template within the original matrix (here, tetra-alkylammonium bromides), pores of larger size,  $d_t$ , are formed after calcination, see Fig. 1(b), which can influence the transport properties (flux and selectivity) of the original membrane. When the amount of template has exceeded some percolation threshold, the larger pores become interconnected throughout the membrane, see Fig. 1(c), and hence the separation properties of the membrane should be determined mainly by these larger pores which present a faster diffusion pathway through the membrane. Increasing the amount of template beyond this limit should ideally influence the porosity and hence flux only, but not the selectivity of the membrane, which should be ideally dependent on the pore size only. However, when an upper limit of template amount is exceeded, the template pores

may aggregate or phase-separate from the embedding matrix, resulting in a compromise of the separation and/or mechanical properties of the templated membrane.

#### 4. Results and discussion

In a first-step, we studied the effect of templating on the transport properties of silica membranes using tetraethylammonium bromide (TEABr) as the pore template. Table 1 presents single-component  $N_2$  and  $SF_6$  permeances at 25 °C of membranes templated with differing amounts of TEABr (TEABr ranged from 2 to 10 wt.% of the silica sol after addition of  $H_2O$  and  $HCl$  to the stock sol but before aging and dilution with ethanol). As seen in the Table, increasing the amount of template results in a marked increase in the  $N_2$  permeance of the membranes while retaining molecular sieving properties as judged by the high  $N_2/SF_6$  selectivity. For the case of membranes prepared without template or with 2 wt.% TEABr, the  $SF_6$  permeance was below the detection limit of the apparatus.

The effect of templating is further demonstrated in Fig. 2 where we plot the permeance at 25 °C of  $CO_2$ ,  $N_2$ ,  $CH_4$  and  $SF_6$  for a 6 wt.% TEABr-silica membrane, prepared with sol of composition (B), and a non-templated silica membrane, prepared with sol of

Table 1  
Single-component  $N_2$  and  $SF_6$  permeances at 25 °C of supports and TEABr-templated silica membranes

Code	Template (wt.%)	$N_2$ permeance ( $mol\ m^{-2}\ s^{-1}\ pa^{-1}$ )	Selectivity $N_2/SF_6$
$\gamma-Al_2O_3$ support	–	$9.5 \times 10^{-6}$	
$\gamma-Al_2O_3 + C_6$ sub-layer	–	$1.4 \times 10^{-6}$	
T0	No template <sup>a</sup>	$1.0 \times 10^{-9}$	– <sup>b</sup>
T2	2	$5.2 \times 10^{-9}$	– <sup>b</sup>
T4	4	$6.7 \times 10^{-8}$	1800
T6	6	$1.8 \times 10^{-7}$	400
T8	8	$2.7 \times 10^{-7}$	92
T10	10	$4.8 \times 10^{-7}$	87

<sup>a</sup> Membrane T0 made with sol of composition (C), all the rest were made with sol (B).

<sup>b</sup>  $SF_6$  permeance below the detection limit of the apparatus.

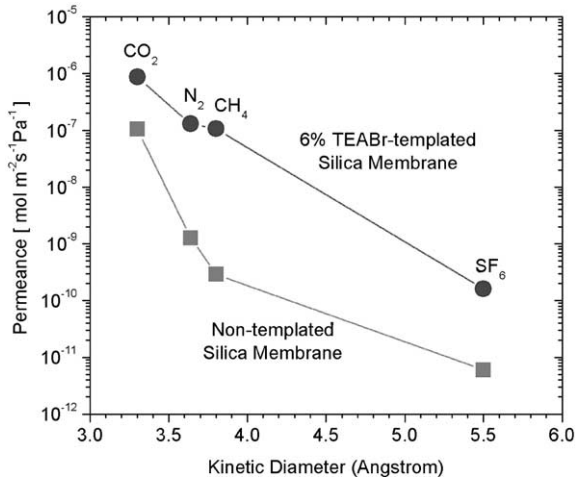


Fig. 2. Single-component permeances vs. kinetic diameter at 25 °C of a 6 wt.% TEABr-templated (●) and a standard, non-templated (■) silica membranes.

composition (C) but without the TEABr template. The non-templated silica membrane is fairly permeable to CO<sub>2</sub> but exhibits a very low permeance of N<sub>2</sub>, CH<sub>4</sub> and SF<sub>6</sub>. In these membranes where no organic template is used, it is believed that water serves as a template creating pores in the range 3.5 Å, thus, resulting in size exclusion for N<sub>2</sub>, CH<sub>4</sub> and larger molecules [14]. On the other hand, the TEABr-templated silica membrane is highly permeable to CO<sub>2</sub>, N<sub>2</sub> and CH<sub>4</sub> but is fairly impermeable to SF<sub>6</sub>, suggesting that it contains pores in the range 4.0–5.5 Å.

After establishing the molecular sieving property of our TEABr-templated membranes with permanent gases, we proceeded with single-component permeation studies of butane isomers, e.g. *n*-butane and *iso*-butane, with kinetic diameters of 4.3 and 5.0 Å, respectively. Table 2 summarizes the transport prop-

Table 2  
Single-component permeances of butane isomers at 30 °C of TEABr-templated silica membranes

Code	Template (wt.%)	<i>n</i> -Butane permeance (mol m <sup>-2</sup> s <sup>-1</sup> Pa <sup>-1</sup> )	Selectivity <i>n</i> -butane/ <i>iso</i> -butane
S2	2	2.5 × 10 <sup>-10</sup>	3.4
S4	4	8.8 × 10 <sup>-9</sup>	40
S6	6	1.0 × 10 <sup>-8</sup>	28
S8	8	1.5 × 10 <sup>-8</sup>	31
S10	10	7.7 × 10 <sup>-8</sup>	22

erties of our membranes for these isomers at 30 °C, as the amount of TEABr is varied in the range 2–10 wt.%. As seen in the table, our membranes exhibit high flux for *n*-butane and high *n*-butane/*iso*-butane selectivity, except for the 2 wt.% TEABr-templated membrane which exhibits very low flux and low selectivity for these isomers. This result suggests that a minimum of ~4 wt.% template is necessary to achieve a percolation threshold as discussed earlier, see Fig. 1. When lower amount of template is used, the butane isomers can hardly diffuse through the membrane since the larger templated pores are not yet interconnected throughout the thickness of the membrane.

Fig. 3 demonstrates the overall molecular sieving property of a 6 wt.% TPABr-templated silica membrane, using single-component permeance data at 80 °C for CO<sub>2</sub>, N<sub>2</sub>, CH<sub>4</sub>, *n*-butane, *iso*-butane and SF<sub>6</sub> [18]. As seen in the figure, this membrane exhibits high permeance for N<sub>2</sub> and *n*-butane coupled with high selectivity for N<sub>2</sub>/SF<sub>6</sub> (460) and *n*-butane/*iso*-butane (14). This further suggests that templated silica membranes possess transport properties similar to those of polycrystalline zeolite MFI membranes made with TPABr as template, where high *n*-butane/*iso*-butane [19] and N<sub>2</sub>/SF<sub>6</sub> [20] selectivities are used as indicators of good membrane quality.

Table 3 summarizes permeation results of different polycrystalline zeolite MFI membranes reported in the literature for the same gas and vapor pairs. It is

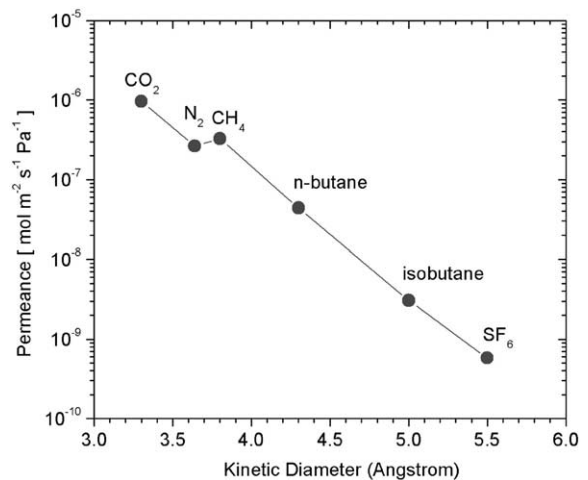


Fig. 3. Single-component permeances vs. kinetic diameter at 80 °C of a 6 wt.% TPABr-templated silica membrane [18].

Table 3  
Transport properties of polycrystalline zeolite MFI membranes

Membrane	$T$ (°C)	Permeance ( $\text{mol m}^{-2} \text{s}^{-1} \text{Pa}^{-1}$ )		Selectivity		Reference
		$\text{N}_2$	<i>n</i> -Butane	$\text{N}_2/\text{SF}_6$	<i>n</i> -Butane/ <i>iso</i> -butane	
Silicalite-1	25	$1.6 \times 10^{-7}$	$1.6 \times 10^{-8}$	10	37	[21]
Silicalite-1	25	$1.5 \times 10^{-7}$	$5.0 \times 10^{-8}$	7	71	[22]
ZSM-5	110	$3.8 \times 10^{-9}$	$1.9 \times 10^{-9}$	610	80	[23]
MFI	25	$1.0 \times 10^{-7}$	$2.7 \times 10^{-8}$	10	84	[24]
H-ZSM-5	25	$2.0 \times 10^{-7}$	$3.4 \times 10^{-8}$	56	20	[25]
ZSM-5	25	$4.3 \times 10^{-7}$	$3.0 \times 10^{-8}$	310	40	[26]
Silicalite-1	25	$7.4 \times 10^{-8}$	$2.0 \times 10^{-8}$	66	54	[27]

noted that the majority of zeolite MFI membranes reported in the literature exhibit *n*-butane/*iso*-butane selectivities in the range of 30–50, while the highest  $\text{N}_2/\text{SF}_6$  selectivities lie in the range 200–300, which are somewhat comparable to respective selectivities obtained with our membranes. At this point, it is emphasized that direct comparison of transport properties even between zeolite MFI membranes reported by different groups is rather difficult because of the differences in thickness, crystal orientation and intercrystalline porosity of membranes fabricated with different experimental protocols. In addition, most zeolite membranes are believed to separate gas or vapor mixtures by differences in both diffusivities and adsorption strengths of mixture components in zeolitic and intercrystalline pores of size  $<10 \text{ \AA}$ , whereas the templated silica membranes reported here appear to discriminate molecules mainly on the basis of size.

After establishing that our organic-templated silica membranes exhibit transport properties similar to those of polycrystalline MFI-type zeolite membranes,

we proceeded with single-component vapor permeation studies using xylene isomers as a model system. The kinetic diameter difference between the smallest and most commercially interesting *para*-xylene ( $d_k = 5.8 \text{ \AA}$ ) and its *meta*- and *ortho*-isomers ( $d_k = 6.8 \text{ \AA}$ ) is large enough and a kinetic separation appears feasible with a molecular sieve membrane with pores in the range 5–6  $\text{ \AA}$  [6]. Indeed, as indicated by the results shown in Table 4, our templated silica membranes exhibit substantial ideal selectivity between *para*- and *ortho*-xylene in the temperature range 30–100 °C and with feed partial pressures in the range 0.7–0.9 kPa for the two isomers. It is noted that permeation measurements at higher temperatures were not attempted because of the limited thermal stability of the epoxy glue used to glaze the tube ends before sealing in the permeation cell.

The xylene transport properties of our amorphous templated silica membranes compare reasonably well with those of respective polycrystalline zeolite MFI membranes reported in the literature. So far,

Table 4  
Single-component xylene permeation properties of templated silica membranes

Code	Template (wt.%)	Temperature (°C)	<i>para</i> -Xylene permeance ( $\text{mol m}^{-2} \text{s}^{-1} \text{Pa}^{-1}$ )	Selectivity ( <i>para</i> -xylene/ <i>ortho</i> -xylene)
M1	TEABr (2)	55	$4.5 \times 10^{-9}$	1.8
M2	TEABr (4)	30	$1.5 \times 10^{-9}$	21.8
M2	TEABr (4)	50	$9.6 \times 10^{-9}$	20.2
M2	TEABr (4)	90	$1.4 \times 10^{-8}$	13.2
M3	TEABr (6)	95	$1.6 \times 10^{-8}$	18.5
M4	TEABr (8)	90	$2.2 \times 10^{-8}$	17.4
M5	TPABr (4)	52	$4.4 \times 10^{-9}$	17.4
M5	TPABr (4)	95	$1.5 \times 10^{-8}$	18.6

Feed partial pressure: *para*-xylene; 0.9 kPa, *ortho*-xylene; 0.7 kPa.

it appears that the best supported MFI membranes are those prepared by a three-step seeding/secondary growth/defect reparation process [6], as judged by reproducible *para*-xylene/*ortho*-xylene selectivities of 30–70 and *para*-xylene flux in the range  $1.0\text{--}2.0 \times 10^{-8} \text{ mol m}^{-2} \text{ s}^{-1} \text{ Pa}^{-1}$ , at a temperature of 125 °C and feed partial pressure conditions similar to those employed here. It is believed that intercrystalline porosity or calcination induced microcracks [6,19,28,29] are responsible for the rather low (<10) *para*-selectivity observed for most of the MFI membranes reported in the literature [30,31], so only very rigorous, multi-step preparation procedures can result in good quality membranes with high selectivities for this isomer system [6]. On the other hand, zeolite membranes with significant amount of non-zeolitic microporosity can still exhibit substantial selectivities for other hydrocarbon isomer systems such as *n*-butane/*iso*-butane or *n*-hexane/2,2-dimethylbutane [5,32] where adsorption properties can favor high selectivity for the smaller linear hydrocarbon.

A main concern in this study is that *para*-xylene/*ortho*-xylene (or *n*-butane/*iso*-butane) single-component selectivities obtained with our amorphous templated silica membranes are not as high as respective values obtained with high-quality, polycrystalline MFI-type zeolite membranes reported in the literature, despite the very high selectivities obtained with permanent gases, e.g. N<sub>2</sub>/SF<sub>6</sub>, see Table 1. This suggests that our amorphous templated silica membranes may possess a distribution of pore sizes around an average, as opposed to crystalline zeolites that possess pores of very precise size, determined by their three-dimensional crystalline lattice. This distribution in pore sizes in our membranes may account for the moderate selectivities observed for the butane or xylene isomers with a small difference in kinetic diameters (0.7–1.0 Å), especially in the case of high amount of template, e.g. see Table 2.

In addition to distributed pore sizes, we suspect that the flexibility of the amorphous silica matrix could be responsible for these moderate selectivities as well, since bulky hydrocarbons such as *iso*-butane or *ortho*-xylene could ‘squeeze’ through micropores and diffuse along the membrane by swelling these pores during their movement through the amorphous silica matrix. Permanent gases, however, may not have this ability and can be easily excluded by a membrane with

pores smaller than their kinetic diameter. This effect could explain the fact that a 2 wt.% TEABr-templated membrane exhibits comparable permeance for N<sub>2</sub> (Table 1) and *ortho*-xylene (Table 4), two molecules of very large difference in size (3.64 versus 6.8 Å). Similar phenomena have also been documented with zeolite MFI in membrane or powder form under certain experimental conditions, where *ortho*-xylene was observed to transport through zeolitic pores with substantial rate [6,19,31] or adsorb at significant loading and distort the crystalline zeolite lattice [33]. At this point, we believe that suitable experimental procedures should be identified in future studies, in order to promote silica matrix densification and reduce framework flexibility, for the purpose of excluding bulky hydrocarbon molecules, such as *iso*-butane or *ortho*-xylene, from entering membrane micropores.

As a final remark, we would like to state that we did not observe substantial differences in the transport properties of membranes templated with either TEABr or TPABr [18]. This suggests that the smallest projected cross-sectional area of the ethyl or propyl ligands of TEABr and TPABr is the critical size that controls permeation, rather than the kinetic diameter of the entire tetra-alkylammonium molecule, which is larger for TPABr. This hypothesis is in agreement with the results of Lu et al. who employed 3-methacryloxypropyl ligand as template of the porosity of their sol-gel silica membranes [17]. In this case, the smallest cross-sectional dimension of the ligand was estimated at ~5.0 Å using molecular simulation, while their membrane was highly permeable for N<sub>2</sub> ( $d_k = 3.64 \text{ \AA}$ ) and propene ( $d_k = 4.5 \text{ \AA}$ ), but essentially impermeable for the larger SF<sub>6</sub> molecule ( $d_k = 5.5 \text{ \AA}$ ). In our case, a high selectivity exhibited by both the TEABr- and TPABr-templated membranes for the linear *n*-butane ( $d_k = 4.3 \text{ \AA}$ ) over its branched *iso*-butane isomer ( $d_k = 5.0 \text{ \AA}$ ) provides further evidence that the minimum aperture that controls selectivity here is the cross-section of the ethyl or propyl ligands of the respective template molecules.

## 5. Conclusions

A simple and effective tetra-alkylammonium-based templating procedure has been demonstrated for preparation of sol-gel silica membranes with pores

in the range 5–6 Å, useful for hydrocarbon isomer separations. These new membranes exhibit gas and vapor transport properties distinctly different from prior solvent-templated silica membranes known in the art, but similar to those of polycrystalline zeolite (e.g. MFI) membranes, as judged by substantial selectivities for N<sub>2</sub>/SF<sub>6</sub>, *n*-butane/*iso*-butane and *para*-xylene/*ortho*-xylene. The unique features of this new approach include simple, fast and scaleable processing under ambient conditions, and the possibility to tune the membrane pore size and porosity by proper choice of the type and amount of template, but at the expense of moderate selectivities as compared to polycrystalline zeolite membranes, due to issues of distributed pore sizes or flexibility of the amorphous silica membrane matrix.

### Acknowledgements

We would like to acknowledge financial support from PPG Industries, Pall Corporation, the UNM/NSF Center for Microengineered Materials and the DOE Basic Energy Sciences Program. Sandia is a multiprogram laboratory operated by Sandia Corporation, a Lockheed Martin Company, for the United States Department of Energy under contract DE-AC04-94AL85000.

### References

- [1] Y.S. Lin, Microporous and dense inorganic membranes: current status and prospective, *Sep. Purif. Technol.* 25 (2001) 39.
- [2] J. Caro, M. Noack, P. Koelsch, R. Schaefer, Zeolite membranes, state of their development and perspective, *Microporous Mesoporous Mater.* 38 (2000) 3.
- [3] R. Lai, G.R. Gavalas, ZSM-5 membrane synthesis with organic-free mixtures, *Microporous Mesoporous Mater.* 38 (2000) 239.
- [4] K. Kusakabe, T. Kuroda, S. Morooka, Separation of carbon dioxide from nitrogen using ion-exchanged faujasite-type zeolite membranes formed on porous support tubes, *J. Membr. Sci.* 148 (1998) 13.
- [5] J. Coronas, R.D. Noble, J.L. Falconer, Separations of C<sub>4</sub> and C<sub>6</sub> isomers in ZSM-5 tubular membranes, *Ind. Eng. Chem. Res.* 37 (1998) 166.
- [6] G. Xomeritakis, Z. Lai, M. Tsapatsis, Separation of xylene isomer vapors with oriented MFI membranes made by seeded growth, *Ind. Eng. Chem. Res.* 40 (2001) 544.
- [7] V. Nikolakis, G. Xomeritakis, A. Abibi, M. Dickson, M. Tsapatsis, D.G. Vlachos, Growth of faujasite-type zeolite membrane and its application in the separation of saturated/unsaturated hydrocarbon mixtures, *J. Membr. Sci.* 184 (2001) 209.
- [8] M. Kondo, M. Komori, H. Kita, K.-I. Okamoto, Tubular-type pervaporation module with zeolite NaA membrane, *J. Membr. Sci.* 133 (1997) 133.
- [9] M.G. Sedigh, L. Xu, T.T. Tsotsis, M. Sahimi, Transport and morphological characteristics of polyetherimide-based carbon molecular sieve membranes, *Ind. Eng. Chem. Res.* 38 (1999) 3367.
- [10] A.B. Fuertes, Preparation and characterization of adsorption-selective carbon membranes for gas separation, *Adsorption* 7 (2001) 117.
- [11] C.J. Brinker, T.L. Ward, R. Sehgal, N.K. Raman, S.L. Hietala, D.M. Smith, D.-W. Hua, T.J. Headley, Ultramicroporous silica-based supported inorganic membranes, *J. Membr. Sci.* 77 (1993) 165.
- [12] C.J. Brinker, R. Sehgal, S.L. Hietala, R. Deshpande, D.M. Smith, D. Loy, C.S. Ashley, Sol-gel strategies for controlled porosity inorganic materials, *J. Membr. Sci.* 94 (1994) 85.
- [13] R.M. de Vos, H. Verweij, Improved performance of silica membranes for gas separation, *J. Membr. Sci.* 143 (1998) 37.
- [14] C.-Y. Tsai, S.-Y. Tam, Y. Lu, C.J. Brinker, Dual-layer asymmetric microporous silica membranes, *J. Membr. Sci.* 169 (2000) 255.
- [15] N.K. Raman, C.J. Brinker, Organic template approach to molecular sieving silica membranes, *J. Membr. Sci.* 105 (1995) 273.
- [16] R.M. de Vos, W.F. Maier, H. Verweij, Hydrophobic silica membranes for gas separation, *J. Membr. Sci.* 158 (1999) 277.
- [17] Y. Lu, G. Cao, R.P. Kale, S. Prabakar, G.P. Lopez, C.J. Brinker, Microporous silica prepared by organic-templating: relationship between the molecular template and pore structure, *Chem. Mater.* 11 (1999) 1223.
- [18] S. Naik, 'Zeolite-like' Silica Membranes for Isomer Separations, M.Sc. Thesis, The University of New Mexico, 1999.
- [19] G. Xomeritakis, S. Nair, M. Tsapatsis, Transport properties of alumina-supported MFI membranes made by secondary (seeded) growth, *Microporous Mesoporous Mater.* 38 (2000) 61.
- [20] J. Coronas, J.L. Falconer, R.D. Noble, Characterization and permeation properties of ZSM-5 tubular membranes, *AIChE J.* 43 (1997) 1797.
- [21] G. Xomeritakis, A. Gouzinis, S. Nair, T. Okubo, M. He, R.M. Overney, M. Tsapatsis, Growth, microstructure and permeation properties of supported zeolite (MFI) films and membranes prepared by secondary growth, *Chem. Eng. Sci.* 54 (1999) 3521.
- [22] W.J.W. Bakker, L.J.P. van den Broeke, F. Kapteijn, J.A. Moulijn, Temperature dependence of one-component permeation through a silicalite-1 membrane, *AIChE J.* 43 (1997) 2203.
- [23] R. Lai, G.R. Gavalas, Surface seeding in ZSM-5 membrane preparation, *Ind. Eng. Chem. Res.* 37 (1998) 4275.

- [24] A.J. Burggraaf, Z.A.E.P. Vroon, K. Keizer, H. Verweij, Permeation of single gases in thin zeolite MFI membranes, *J. Membr. Sci.* 144 (1998) 77.
- [25] V.A. Tuan, J.L. Falconer, R.D. Noble, Alkali-free ZSM-5 membranes: preparation conditions and separation performance, *Ind. Eng. Chem. Res.* 38 (1999) 3635.
- [26] C.J. Gump, X. Lin, J.L. Falconer, R.D. Noble, Experimental configuration and adsorption effects on the permeation of C<sub>4</sub> isomers through ZSM-5 zeolite membranes, *J. Membr. Sci.* 173 (2000) 35.
- [27] M. Nomura, T. Yamaguchi, S.-I. Nakao, Silicalite membranes modified by counter-diffusion CVD technique, *Ind. Eng. Chem. Res.* 36 (1997) 4217.
- [28] K. Wegner, J. Dong, Y.S. Lin, Polycrystalline MFI zeolite membranes: xylene pervaporation and its implication on membrane microstructure, *J. Membr. Sci.* 158 (1999) 17.
- [29] J. Dong, Y.S. Lin, M. Hu, R.A. Peascoe, E.A. Payzant, Template-removal-associated microstructural development of porous-ceramic-supported MFI zeolite membranes, *Microporous Mesoporous Mater.* 34 (2000) 241.
- [30] C.D. Baertsch, H.H. Funke, J.L. Falconer, R.D. Noble, Permeation of aromatic hydrocarbon vapors through silicalite-zeolite membranes, *J. Phys. Chem.* 100 (1996) 7676.
- [31] C.J. Gump, V.A. Tuan, R.D. Noble, J.L. Falconer, Aromatic permeation through crystalline molecular sieve membranes, *Ind. Eng. Chem. Res.* 40 (2001) 565.
- [32] C.J. Gump, R.D. Noble, J.L. Falconer, Separation of hexane isomers through non-zeolite pores in ZSM-5 zeolite membranes, *Ind. Eng. Chem. Res.* 38 (1999) 2775.
- [33] S. Nair, M. Tsapatsis, The location of *o*- and *m*-xylene in silicalite by powder X-ray diffraction, *J. Phys. Chem. B* 104 (2000) 8982.